# Evaluation of the protective effect of Compound Kushen Injection against radiation-induced lung injury in mice

TING XU[1], SHARMISTHA CHAKRABORTY[2], DAOYAN WEI[3], MEGAN TRAN[2],
ROBYN RHEA[2], BO WEI[4], PHUONG NGUYEN[2], MIHAI GAGEA[5], XIAOXUE XIE[1,6],
LIRONG WU[1,7], LORENZO COHEN[2], ZHONGXING LIAO[1] and PEIYING YANG[2]

[1]Division of Radiation Oncology, The University of Texas MD Anderson Cancer Center, Houston, TX 77030, USA;
[2]Department of Palliative, Rehabilitation and Integrative Medicine, The University of Texas MD Anderson Cancer Center,
Houston, TX 77030, USA; [3]Department of Gastroenterology, Hepatology and Nutrition, The University of Texas MD Anderson
Cancer Center, Houston, TX 77030, USA; [4]Department of Bioinformatics and Computational Biology, The University of
Texas MD Anderson Cancer Center, Houston, TX 77030, USA; [5]Department of Veterinary Medicine and Surgery,
The University of Texas MD Anderson Cancer Center, Houston, TX 77030, USA

**Abstract.** Radiation-induced lung injury (RILI) is a prevalent complication following thoracic radiation, and currently there is a lack of effective intervention options. The present study investigated the potential of Compound Kushen Injection (CKI), a botanical drug, to mitigate inflammatory responses in mice with RILI, along with its underlying mechanisms of action. C3H mice underwent total lung irradiation (TLI) and intraperitoneal injection of CKI (2, 4 or 8 ml/kg) once daily for 8 weeks. Pre-radiation treatment with 4 or 8 ml/kg CKI starting 2 weeks before TLI or concurrent treatment of 8 ml/kg CKI with TLI led to a significantly longer overall survival compared with the TLI vehicle-treated group. Micro-computed tomography evaluations showed that concurrent treatment with 8 ml/kg CKI was associated with a significantly lower incidence of RILI. Histological evaluations revealed that concurrent CKI (4 and 8 ml/kg) treatment significantly reduced grades of lung inflammation. Following radiation at 72 h, TLI plus vehicle-treated mice had significantly elevated serum IL6, IL17A, and transforming growth factor β (TGF-β) levels compared with non-irradiated normal mice. Conversely, mice that received TLI plus CKI displayed lower cytokine levels than those in the TLI plus vehicle-treated mice. Immunohistochemistry staining showed a reduction of TGF-β positive cells in the lung tissues of TLI mice after CKI treatment. The concurrent TLI CKI-treated mice had a significantly reduced cyclooxygenase 2 (COX-2) activity and COX-2 metabolites compared with TLI vehicle-treated mice. These data highlight that CKI substantially reduced radiation-induced lung inflammation, mitigated RILI incidence, and prolonged overall survival.

*Correspondence to:* Dr Peiying Yang, Department of Palliative, Rehabilitation and Integrative Medicine, The University of Texas MD Anderson Cancer Center, 1515 Holcombe Boulevard, Unit 1414, Houston, TX 77030, USA
E-mail: pyang@mdanderson.org

Dr Zhongxing Liao, Division of Radiation Oncology, The University of Texas MD Anderson Cancer Center, 1515 Holcombe Boulevard, Unit 1422, Houston, TX 77030, USA
E-mail: zliao@mdanderson.org

*Present address:* [6]Hunan Key Laboratory of Translational Radiation Oncology, Hunan Cancer Hospital, The Affiliated Cancer Hospital of Xiangya School of Medicine, Central South University, Changsha, Hunan, 410006, P.R. China; [7]Department of Radiation Oncology, Jiangsu Cancer Hospital & Jiangsu Institute of Cancer Research & The Affiliated Cancer Hospital of Nanjing Medical University, Nanjing, Jiangsu, 210009, P.R. China

## Introduction

Radiation-induced lung injury (RILI) is common in patients with lung cancer treated with thoracic radiation and is symptomatic in 15 to 40% of patients (1-4). The median time to development of symptomatic RILI is 4-6 months after completion of chemoradiation with a range from the end of radiation up to 12 months (5). RILI can cause multiple symptoms including shortness of breath, fever, chest pain, cough, hypoxia, and respiratory failure, or even death, which significantly impacts quality of life and negatively affects survival (6). At the tissue level, RILI presents as increased infiltration of inflammatory

cells and fluid accumulation in alveoli, interstitial edema, epithelial degeneration followed by regeneration, bronchial epithelium intrusion into the alveoli, disruption of endothelial integrity and microvasculature and atelectasis (7). RILI mainly includes radiation pneumonitis (RP) and radiation lung fibrosis (RF). RP is the acute phase of RILI which usually developed within 6 months after radiation and often progresses to irreversible chronic fibrosis (4), resulting in decreased pulmonary function and hypoxia, which significantly impacts patients' quality of life (8,9). For patients with RILI requiring intervention, steroids and supplemental oxygen are the only reliable treatments, as no effective drug specifically mitigates RILI. Amifostine is among the most extensively investigated thiols for protecting normal tissue from various cancer therapies. However, its clinical use in RILI prevention has not gained popularity owing to its high incidence of side effects (10) and high variability of therapeutic effects in clinical trials (11). The absence of effective therapeutic remedies for RILI represents a significant unmet clinical need.

The progressive dysregulation of lung tissue caused by RILI can begin immediately after radiation exposure, driven by the production of free radicals, increased oxidative stress, and an associated inflammatory cytokine response (12). Two primary mechanisms trigger radiation-induced tissue injuries: DNA double-strand breaks and the generation of reactive oxygen species (13,14). In addition, radiation-induced damage to DNA or cytoplasmic organelles activates intracellular signaling that leads to altered gene expression (15). Many cytokines and chemokines are elevated in the circulating blood, bronchoalveolar fluid, or lung tissues of humans and mice with RILI (16-19). For example, IL6, showed a persistent elevation in mouse lung tissues after irradiation, coinciding with the onset of acute pneumonitis (19). Transforming growth factor β (TGF-β), derived from inflammatory cells and, to a lesser extent, from pneumocytes and fibroblasts, is a key cytokine involved in the fibrotic process (8,20-22). Rube *et al* (22) reported that TGF-β elevation in lung tissue could be induced by 12 Gray (Gy) thoracic radiation, with TGF-β expression predominantly localized in areas of inflammatory cell infiltrates and fibrosis. Elevated circulating IL-6 and TGF-β during and after radiation were predictive of RILI in thoracic cancer patients (21,23,24). More recently, studies showed that RILI can be induced through the activation of the IL6-TGFβ-IL17 pathway (25-27).

Furthermore, one of the predominant histopathological events in RILI is local inflammation. Cyclooxygenase 2 (COX-2) plays an essential role in RILI by producing prostaglandin (PG). Selective COX-2 inhibitors, such as celecoxib, have been shown to significantly improve the survival of irradiated mice when treatment started 9 weeks after radiation, suggesting the importance of COX-2 pathway in mitigating radiation induced RILI (28). Another study reported Psoralidin, a dual inhibitor of COX-2 and 5-LOX, inhibited the IR-induced COX-2 expression and PGE (2) production, further demonstrating the importance of COX-2-mediated inflammatory pathway in RILI (29). Thus, we explored alterations in the COX-2 pathway in RILI mouse models in the current study.

Compound kushen injection (CKI) is a hot water extract from the herbs kushen (*Sophora flavescentis radix*) and baituling (*Heterosmilax yunnanensis rhizoma*). Kushen has long been used in China to treat tumors, inflammation, and other diseases, including viral hepatitis, enteritis, viral myocarditis, arrhythmia, and skin diseases (e.g., colpitis, psoriasis, eczema) (30). The major bioactive components of kushen are matrine and oxymatrine. CKI is manufactured in a GMP-compliant facility and contains over 200 different chemical components, predominantly alkaloids and flavonoids, primarily derived from kushen (31).

As a product approved by the Chinese Food and Drug Administration, CKI has been regularly used in oncology clinics in China for more than 20 years (30,32,33). It has been used in combination with chemotherapy for treating gastric, liver, and non-small cell lung carcinomas (34) and has also been observed to alleviate the toxicity of radiochemotherapy (35). Treatment regimens include 12-30 ml intravenous injection daily for 4-8 weeks and is provided concurrently in patients getting radiotherapy (30,32,33). In a systematic review and meta-analysis of 13 clinical studies, Wang *et al* (32) reported that CKI significantly reduced radiation-induced adverse events, including radiation pneumonitis, esophagitis, and bone marrow suppression, and improved quality of life in non-small cell lung cancer patients. Most recently, a study conducted in China documented CKI's efficacy in reducing the incidence of grade ≥2 RILI, alleviating symptom burden, and improving quality of life in lung cancer patients (36). However, a limitation is that all the prior clinical research was conducted in China.

Preclinical research on CKI shows that its treatment induces cell cycle arrest and autophagic cell death by upregulation of LC3-I and II protein expression in human NSCLC H1975 and H1650 cells, while also sensitizing these cells to gefitinib by down regulation of PI3K/mTOR pathways (37,38). The effect of CKI on apoptosis was also reported in breast cancer MCF-7 and liver cancer HepG2 cells (39). CKI inhibits sarcoma growth and tumor-induced hyperalgesia via TRPV1 signaling pathways and suppresses human breast cancer stem-like cells by downregulating the canonical Wnt/β-catenin pathway (40). However, CKI's mechanisms regarding its effects on RILI are still under investigation, representing a significant knowledge gap.

Thus, the goal of the present study aimed to assess the effects of CKI treatment on RILI in mouse models and to unravel its underlying mechanism of action. Our hypothesis was centered on CKI's potential to mitigate RILI via its anti-inflammatory effect, suggesting its prospective application for patients at risk of developing RILI.

## Materials and methods

All procedures were performed according to the relevant guidelines, rules, and regulations of The University of Texas MD Anderson Cancer Center.

*Study drug*. CKI (batch #20180301 or #20200110) was provided by Shanxi Zhendong Pharmaceutical Co. (Changzhi, Shanxi, China); it was manufactured using the same procedures as those used to manufacture the CKI product that is used in the clinical setting in accordance with good manufacturing practices (36). Every 1 ml of CKI is standardized to

contain 8.0 to 14.0 mg of matrine and oxymatrine, and 0.35 to 1.20 mg of macrozamin. Fig. S1 shows the quantification and consistency of matrine and oxymatrine in three batches of CKI, two of which were used in this study, analyzed by High performance liquid chromatography with tandem mass spectrometry (LC-MS/MS). Total volumes of 200 $\mu$l solutions were prepared for each injection with CKI and saline. The amount of CKI included in each injection at doses of 2, 4 and 8 ml/kg were 50, 100 and 200 $\mu$l of CKI, diluted with 150, 100, and 0 $\mu$l of saline, respectively.

*Other materials*. Prostaglandin E$_2$ (PGE$_2$), PGD$_2$, and its relevant internal standards PGE$_2$-d4 and PGD$_2$-d4, as well as COX-2 activity assay kit (#760151) were purchased from Cayman Chemical (Ann Arbor, MI). Anti-Cyclooxygenase-2 (Anti-COX-2) and anti-15-hydroxyprostaglandin dehydrogenase (anti-15-PGDH) antibodies were obtained from Novus Biological (Centennial, CO).

*Animals*. Female C3H/KamL mice from the Department of Experimental Radiation Oncology, MD Anderson and female C3H/heN mice (Charles River, Wilmington, MA) were used in this study. As described previously, the C3H mouse strain is well characterized in studies of RILI intervention (28,41). The study mice were 12 to 16 weeks old. They were housed at the institutional animal facility under controlled temperature and humidity levels and a 12:12 h light-dark schedule. They were given lab chow diet (Harlan Laboratories, Indianapolis, IN) and water ad libitum. Mice were euthanized by CO$_2$ inhalation when they lost 20% of body weight or became moribund. Exposure to CO$_2$ was performed in the home cage. The CO$_2$ was gradually increased, with a CO$_2$ asphyxiation rate of 30-70% of chamber volume per min.

*Radiation procedure*. Total lung irradiation (TLI) was performed using an XRAD 225Cx (Precision X-Ray, North Branford, CT). Irradiation was performed according to the standard operating procedure of our institution's Small Animal Imaging Facility. The setup for TLI consisted of a 225 kVp, 13.3 mA beam with a 0.15 mm copper filter and 20x20 mm beam collimator. Radiation was delivered at a dose rate of 300 Gy/min from the anterior-posterior/posterior-anterior direction using two parallel opposing beams. Mice were anesthetized with inhaled anesthesia (5% isoflurane for induction and 1.5-3% for maintenance) and positioned so that only the thorax was exposed in the radiation field.

*Experiments*
*Experiment 1: determine the optimal timing and dose response of CKI treatment after a single dose radiation exposure, focusing on its impact on survival*. A single radiation dose of 13.5 Gy was used to determine the efficacy of CKI in preventing RILI and its relevant mechanism of action, as a previous study showed that C3H mice developed pneumonitis after they were irradiated at this dose level (28,42,43). The optimal timing of CKI delivery was investigated using three different schedules: 1) starting 2 weeks prior to TLI; 2) starting concurrently on the same day as TLI; or 3) starting 9 weeks after TLI, which is the median time for the development of acute RILI (see treatment schema in Fig. 1A). When

CKI and TLI were given on the same day, mice were irradiated before receiving CKI treatment.

CKI was administered to mice (n=16 to 20 per dose group) once per day five days/week via intraperitoneal injection at doses of 2, 4, or 8 ml/kg for a total of 8 weeks (40 injections), with a 1-week break after the initial 4 weeks. The treatment schedule was based on the CKI administration schedule routinely used in oncology clinics in China. The 4 ml/kg dose was equivalent to a clinical dose of 20 ml/day, which is the dose approved by the China Food and Drug Administration for this product (32,33).

Blood was collected from the facial vein at 2, 4, 8 weeks after TLI. Micro-computed tomography (CT) imaging was performed 1 week before and 4-12 weeks after TLI. Lung tissues were collected and processed for histopathological evaluation at the termination of the study. Survival and RILI were evaluated and compared between the treatment groups to determine the optimal timing and dose of CKI.

*Experiment 2: determine the effect of CKI on survival at different radiation dose levels*. Mice were randomly assigned to TLI only and TLI + CKI groups. Mice were irradiated at a range of single radiation doses (11.75-14 Gy, n=3 to 9 per group) to establish radiation dose response on survival. In the TLI + CKI group, CKI 8 ml/kg was injected to mice concomitantly with TLI and then daily for 8 weeks, as this was the most effective dose and schedule suggested from the results of experiment 1.

*Experiment 3: Determine the potential mechanisms of CKI in mitigating RILI*. To investigate the potential mechanism(s) for the effects of CKI at reducing RILI, experimental mice (n=3-8 per group) were treated with 13.5 Gy TLI and CKI at doses of 4 and 8 ml/kg CKI concomitantly and daily for 8 weeks. Mice treated with saline ± TLI were used as blank control groups. Blood was drawn from the facial vein at 72 h for cytokine analysis. Micro-CT imaging and lung tissue collections were performed at 2, 4, 6, and 8 weeks after TLI for RILI evaluation. In addition, lung tissues were either formalin-fixed or flash frozen for related experiments.

*Endpoints evaluations*
*Survival evaluation*. The primary endpoint of this study was mouse survival. Mice were weighed weekly and observed daily for signs of morbidity (hunched posture, progressive weight loss exceeding 20%, or labored breathing). Mice were euthanized by CO$_2$ inhalation when they lost more than 20% of their body weight or became moribund.

*RILI evaluation*
*Micro-CT imaging evaluation*. Micro-CT imaging was performed using XRAD 225Cx (Precision X-Ray) within 1 week before radiation and again 1-3 months after radiation. Briefly, the mice were anesthetized with inhaled anesthesia (5% isoflurane for induction and 1.5-3% for maintenance). When the mice were fully anesthetized, a 22-gauge endotracheal tube was placed using a BioLite mouse intubation system (Braintree Scientific, Braintree, MA). The CT parameters used were 60 kV, 4 mA, and 3 rpm. The mice were mechanically ventilated at 60 breaths per min throughout the procedure, and

a 20-sec breath hold was applied during image acquisition at 20 cmH$_2$O. The pressure was monitored through an inline manometer. After image acquisition was complete, the mice were extubated and recovered in a clean and warm cage. Two to three certified radiation oncologists blinded to experiment groups reviewed the Micro-CT images for RILI evaluation.

*Histopathology evaluation*. Formalin-fixed lung tissues were embedded in paraffin, and sections were stained with hematoxylin and eosin (H&E) for histopathological examination. The RILI score was established based on the evaluation of H&E-stained lung sections as follows: grade 1, minimal tissue changes affecting 1 to 10% of the tissue; grade 2, mild tissue changes affecting 11 to 20% of the tissue; grade 3, moderate tissue changes affecting 21 to 40% of the tissue; and grade 4, marked tissue changes affecting 41 to 100% of the tissue. A certified veterinary pathologist blinded to experimental groups performed histopathological examinations of 4-5 lung tissues from each lobe.

*Immunohistochemistry*. Formalin-fixed lung tissues were embedded in paraffin, and sections were stained with COX-2 (Cell Signaling, #12282) or TGF-β (Abcam, Waltham, MA) antibodies for immunohistochemistry (IHC) analyses. For the IHC staining, 4-$\mu$m sections were stained following the standard operating procedure of our institution's histopathological core facility. The stained slides were scanned with an Aperio AT2 bright-field slide scanner (Durham, NC), and IHC staining was quantified with Aperio image analysis algorithms for each lobe of the lung tissues (44).

*Serum cytokine analysis*. Given that proinflammatory cytokines, including IL6, IL17, and TGF-β have been associated with RILI and that changes in these cytokines appeared soon after radiation in C3H mice (16,17), the serum levels of these cytokines were determined by enzyme-linked immunosorbent assay (ELISA) kits (R&D Systems, Minneapolis, MN, or Invitrogen/Thermo Fisher Scientific, Waltham, MA).

*COX-2 activity in lung tissue*. Lung tissues were homogenized with cold buffer containing 0.1M Tris pH 7.8 and 1 mM EDTA (10 ml/g of tissue). COX-2 activity was assessed according to the manufacture instruction. Briefly, the lung tissue supernatants were collected and used for the assay. An aliquot of 40 ml lung tissue supernatant was mixed with 10 ml of Hemin, 20 ml of Colorimetric substrate, and 20 ml of arachidonic acid in 110 ml of assay buffer. The absorbance was read at 590 nM. COX-2 activity was calculated by subtracting an average background sample and from its corresponding sample or inhibitor treated sample. COX-2 activity was calculated per sample using TMPD extinction coefficient of 0.00826 mM$^{-1}$ following instructions from the manufacturer (Cayman Chemical, #760151).

*Eicosanoid-profiling analysis*. We and others have demonstrated the importance of COX-2-mediated inflammatory mediators in RILI (28,29), thus, we further determined the levels of cyclooxygenase metabolites in lung tissue using LC-MS/MS method, as described previously (45). Briefly, analyses were performed using an Agilent 6460 Triple Quadrupole mass spectrometer (Santa Clara, CA) equipped with an Agilent 1200 HPLC system. Eicosanoids were separated using a Kinetex C18 2.6-$\mu$m, 2.0x100-mm column (Phenomenex, Torrance, CA). The mobile phases used 0.1% formic acid in water (phase A) and 0.1% formic acid in acetonitrile (phase B). For the analyses of prostaglandins PGE$_2$ and PGD$_2$, separation was achieved using a linear gradient of 20-98% of 0.1% formic acid in acetonitrile (phase B) with a total time of 33 min. The flow rate was 400 $\mu$l/min with a column temperature of 30°C. The sample injection volume was 15 $\mu$l. Samples were kept at 4°C during the analysis. The mass spectrometer was operated in the electrospray negative-ion mode with a gas temperature of 350°C, a gas flow rate of 10 l/min, and a nebulizer pressure of 20 psi. The temperature of the sheath gas was 350°C and the sheath gas flow rate was 12 l/min. The capillary voltage was -2,900 V. Fragmentation was performed for all compounds, using nitrogen as the collision gas. COX-2 metabolites were detected using electrospray negative ionization and multiple-reaction monitoring of the transitions at mass-to-charge ratios of 351.2 →271.2 for PGE$_2$/PGD$_2$ and 355.2 →275.2 for PGE$_2$-d4/PGD$_2$-d4. The results were expressed as nanograms of prostaglandins per milligram of protein.

*Immunoblotting*. Frozen lung tissue samples were washed with cold PBS and homogenized in lysis buffer containing proteinase and phosphatase inhibitor cocktails with Precellys homogenizer (Bertin Technologies, Montigny-le-Bretonneux, France). The tissue lysates were collected after being centrifuged at 16,000 rpm in 4°C. The immunoblotting was performed using the automated western blotting system. The Jess™ Simple Western system (ProteinSimple, San Jose, CA, USA,) is a system that automatically separates and immunodetects proteins by size through its capillaries. To quantify the interested protein expression, the standard method for 12-230-kDa Jess separation module (SM-W004) was followed. The final protein concentration of tissue lysate (0.4 to 1 mg/ml) was obtained by mixing measured tissue lysate (0.6 to 2 mg/ml) with 0.1X Sample buffer and Fluorescent 5X Master mix (ProteinSimple). This mixture was denatured at 95°C for 5 min. Primary antibodies of interest (COX-2 and 15-PGDH) and tubulin were prepared by mixing antibody diluent with ratio from 1:10 to 1:50. Secondary antibodies were prepared by combining chemiluminescence antibody and fluorescence antibody. After that, tissue lysate samples were loaded into the Ladder (12-230-kDa) plate, followed by the loading of antibody diluent, primary antibody, secondary antibody, luminol-s and peroxide mixture (for chemiluminescence detection), and wash buffer according to the manufacturer instruction. Digital images of chemiluminescence and fluorescence of the interested proteins were captured with Compass Simple Western software (version 4.1.0, Protein Simple), and the area was used for the quantification of the proteins.

*Statistical analyses*. Kaplan-Meier survival functions and log-rank tests were performed to compare survival durations between the treatment groups. RILI incidence rates were compared between the control and CKI-treatment groups using the Fisher's exact test. Differences in histopathologic pneumonitis grade score and protein expression levels were
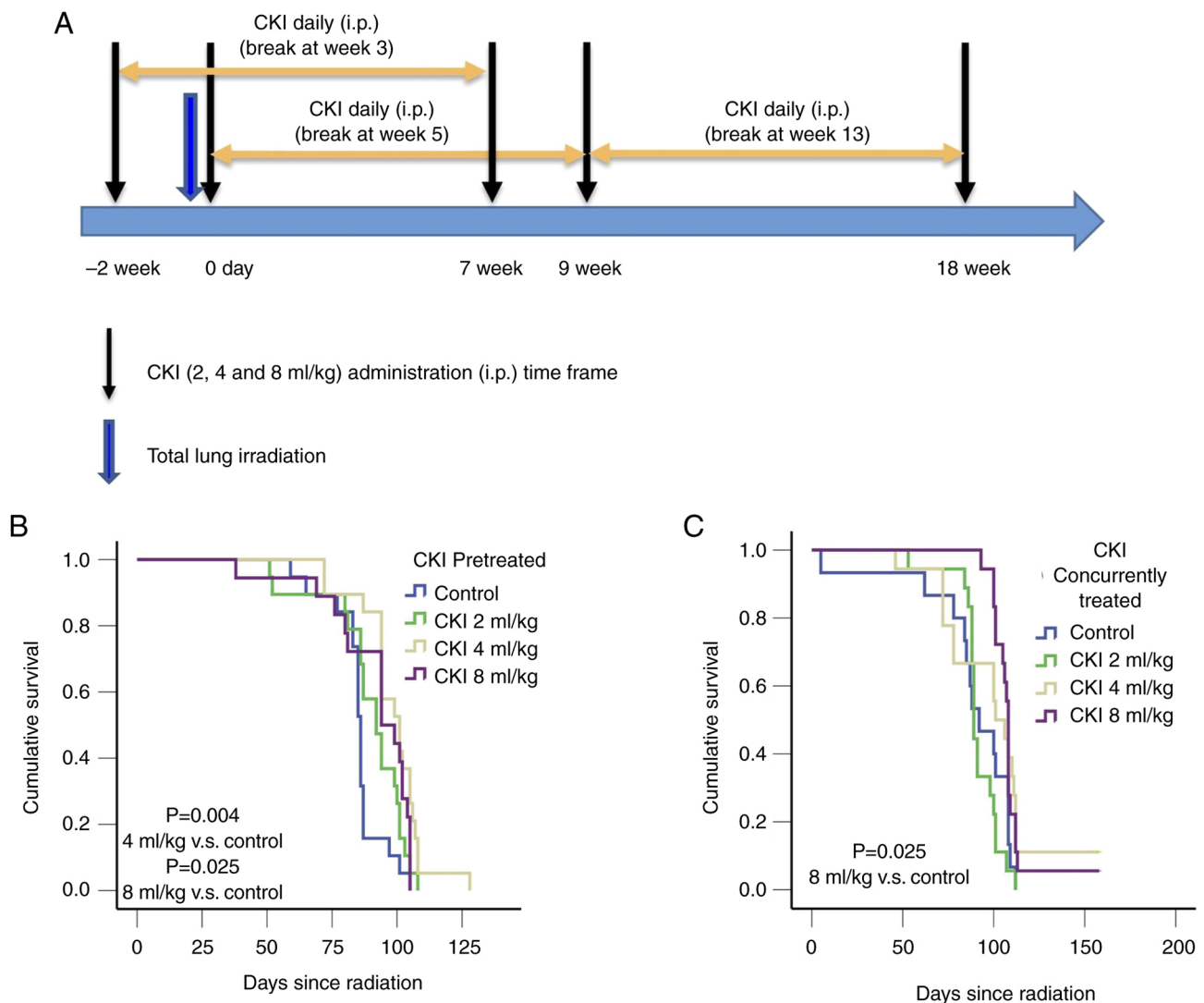
Figure 1. Treatment schema and Kaplan-Meier survival analysis of C3H mice treated with CKI. (A) Illustration of the treatment delivery schedules. Two cycles (5 days a week for 4 weeks/cycle), separated by a week, of CKI were given to the study mice through i.p. injection. Three different administration schedules of CKI were tested, including starting CKI 2 weeks before TLI, starting it concomitantly with TLI and starting it 9 weeks after TLI. The total lung of C3H mice were exposed to a single 13.5 Gy dose and treated with the indicated doses of CKI. (B) Survival curves for C3H mice treated with CKI before irradiation (4 ml/kg CKI vs. control, P=0.004; 8 ml/kg CKI vs. control, P=0.025). (C) Survival curves for irradiated mice treated with CKI starting at the time of irradiation (8 ml/kg CKI vs. control, P=0.025). CKI, Compound Kushen Injection; i.p., intraperitoneal injection; TLI, total lung irradiation.

compared using the two-sample independent t-test. Data distribution of normality was tested by Shapiro-Wilk test. If not normal, log transformation was performed for analysis. The statistical significance threshold was P<0.05. Statistics were performed by SPSS version 29.0 (IBM Corp., Armonk, NY) and GraphPad Prism version 10 (GraphPad Software Inc., Boston, Massachusetts USA).

## Results

*CKI improved survival of C3H mice after TLI.* CKI was given to irradiated C3H mice according to three different schedules as shown in Fig. 1A. Mice that received pre-treatment CKI at 4 ml/kg (101.0±5.0 days, P=0.004) and 8 ml/kg (94.0±7.6 days, P=0.025; Fig. 1B) had significantly longer median survival compared with the vehicle (saline) control mice (86.0±0.8 days). Similarly, mice that received 8 ml/kg CKI concurrently had 16 days longer median survival compared with the vehicle

control mice (108.0±0.4 days vs. 92.0±8.4 days, P=0.025 Fig. 1C). However, mice that received 4 ml/kg CKI concurrently did not show survival benefit over the control group (101.0±6.4 vs. 92.0±8.4 days, P=0.126; Fig. 1C). There was no significant benefit in survival for 2 ml/kg CKI regardless of when the CKI was administered (Fig. 1B and C). Additionally, there were no significant differences in survival of the mice treated with CKI at 9 weeks after TLI (Fig. S2).

To further understand whether the protective effect of CKI against RILI depends on the given dose of radiation, we examined the effect of CKI on RILI in C3H mice that received radiation doses of 11.75, 12.5, 13.25, or 14 Gy. Mice that received 14 Gy radiation had significantly shorter median survival (median ± SE: 86.0±1.8 days, P<0.05; Fig. 2A) than the mice that received 11.75 or 12.5 Gy only (median ± SE: 94.0±0.8 and 98±5.7 days respectively). The three lower radiation dose only groups, 11.75, 12.5, and 13.25 Gy, did not show differences in survival between each other (median survival
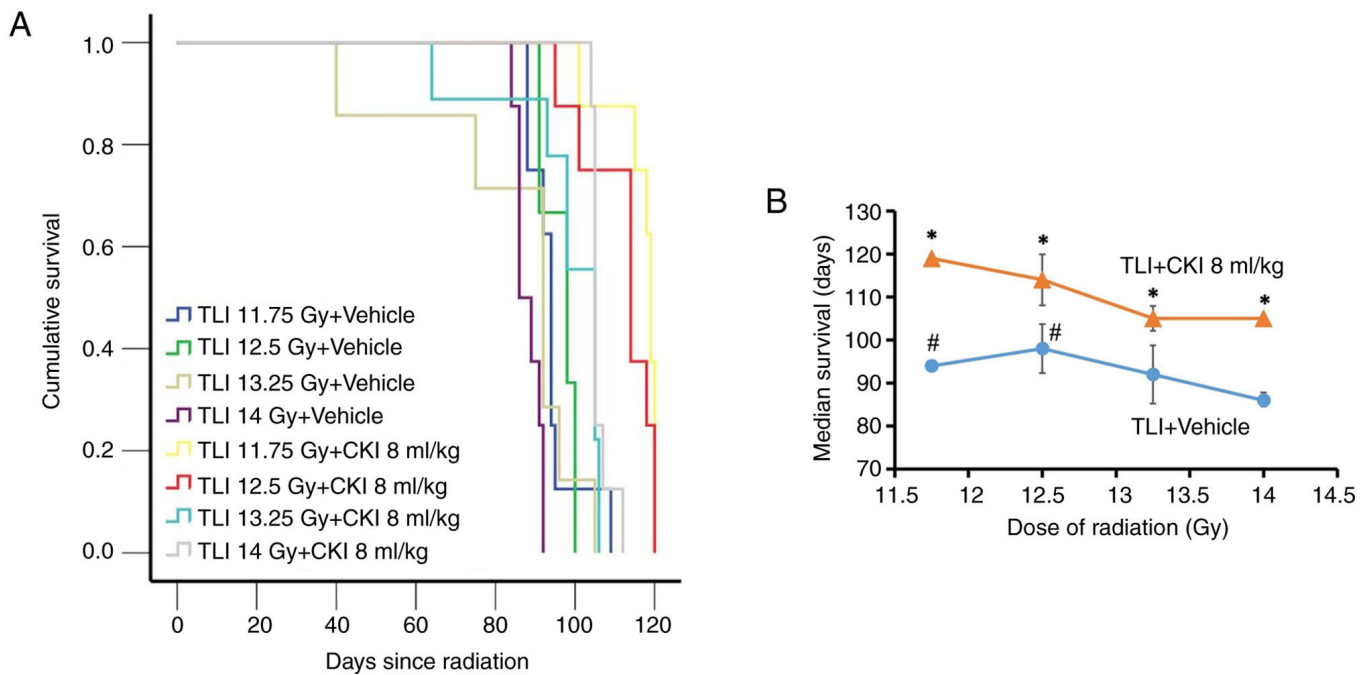
Figure 2. Dose-dependent overall survival of C3H mice. (A) Kaplan-Meier curves for TLI + vehicle and TLI + 8 ml/kg CKI-treated mice at radiation dose levels ranging from 11.75 to 14 Gy. (B) Median survival times for TLI + vehicle and TLI + 8 ml/kg CKI-treated mice at radiation dose levels from 11.75 to 14 Gy. The median survival times of TLI + vehicle-treated mice were significant longer at the two lowest radiation doses (11.75 and 12.5 Gy) compared to those at the highest radiation dose (14 Gy). CKI treatment (8 ml/kg) significantly prolonged the median survival times of irradiated mice compared to vehicle-treated mice at all radiation dose levels. [#]$P<0.05$ vs. TLI (14 Gy) + vehicle. [*]$P<0.05$ vs. TLI + vehicle at the same radiation dose level. CKI, Compound Kushen Injection; TLI, total lung irradiation.

time: 92 to 98 days). We found that concurrent 8 ml/kg CKI treatment significantly increased survival in all radiation dose levels with median survival prolonged by 13-25 days ($P<0.05$, Fig. 2B). These results suggest that CKI exerted protection against RILI-associated mouse death within a defined dose of radiation from 11.75 to 14 Gy.

*CKI decreased the incidence of RILI in C3H mice after TLI.* Micro-CT imaging of lung tissues was performed before and 1-3 months after concurrent 13.5 Gy TLI and CKI treatment to monitor RILI. Representative micro-CT images showed lung tissues in non-irradiated normal condition (Fig. 3Aa), subsequent severe whole lung RILI with airspace consolidation after TLI + vehicle treatment (Fig. 3Ab), moderate RILI with ground-glass opacities in both lungs (indicated by white arrows) after TLI + CKI 8 ml/kg treatment (Fig. 3Ac), and no RILI after TLI + CKI 8 ml/kg treatment (Fig. 3Ad). Both 4 ml/kg (n=8) and 8 ml/kg (n=13) CKI treatment groups had lower incidences of RILI than that of the vehicle control group (n=5) with RILI rates of 25% (4 ml/kg, P=0.086) and 8% (8 ml/kg, P=0.008) vs. 80% (vehicle) (Fig. 3B). To further investigate the differences in pathological changes occurred in TLI + vehicle vs. TLI + CKI groups, a certified veterinary pathologist blinded for experiment groups performed histopathological examinations of the formalin-fixed lung tissues. The lung tissues from CKI treated non-irradiated mice (Fig. S3) had similar histologic appearance with vehicle treated non-irradiated mice (Fig. 4Ad), suggesting CKI itself did not affect the lung histology in normal C3H mice. Histopathologic evaluation of lung tissues revealed that the
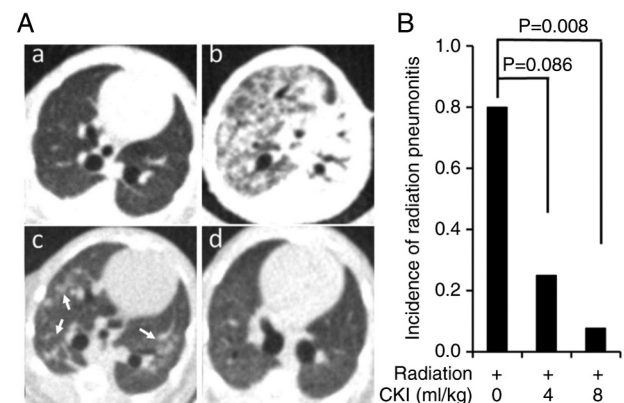


Figure 3. RILI incidence in TLI-treated C3H mice. Micro-CT imaging was conducted to estimate lung tissue damage and the protective effects of CKI treatment in mice 4 to 12 weeks after radiation of 13.5 Gy. (A) Representative micro-CT images of lung tissues from: (a) Normal, nonirradiated mice; (b) mice treated with TLI + vehicle that developed whole lung RILI; (c) mice treated with TLI + 8 ml/kg CKI that developed moderate RILI (indicated by white arrows); and (d) mice treated with TLI + 8 ml/kg CKI that did not develop RILI. (B) Incidence of RILI in mice treated with TLI + vehicle control, TLI + 4 ml/kg CKI, and TLI + 8 ml/kg CKI. RILI, radiation-induced lung injury; TLI, total lung irradiation; CKI, Compound Kushen Injection; CT, computed tomography.

TLI + vehicle control group had marked acute interstitial pneumonia, represented by diffuse alveolar infiltration of many inflammatory cells (neutrophils and macrophages, black arrow), and edema with abundant intra-alveolar exudation of proteinaceous fluid forming hyaline membranes (green arrow)
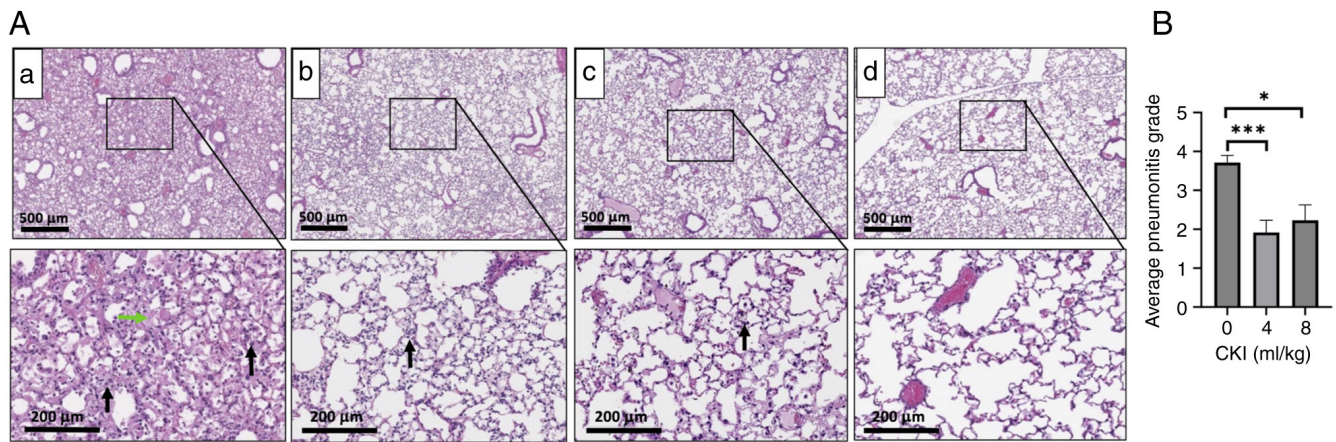
A



B



Figure 4. Histopathological analysis of lung tissue from TLI mice. (A) Images of hematoxylin and eosin stained lung tissues at 5x and 20x magnifications obtained from C3H mice at termination of the study. (a) TLI + vehicle control mouse showing lung with marked interstitial pneumonitis-with alveolar infiltration of many inflammatory cells (black arrow) and edema with abundant exudation of eosinophilic proteinaceous fluid into the alveolar spaces making thick hyaline membranes along the alveolar walls (green arrow); (b) TLI + 4 ml/kg CKI and (c) TLI + 8 ml/kg CKI-treaded mice showing comparable mild and minimal interstitial pneumonitis with alveolar infiltration of inflammatory cells (black arrow); (d) normal lung tissue from vehicle treated non-irradiated mouse. (B) Mean pneumonitis grades in mice treated with TLI plus 0, 4, or 8 ml/kg CKI (n=7-13 per group). Data are presented as the mean ± standard error. $^*$P<0.05 and $^{***}$P<0.001. TLI, total lung irradiation; CKI, Compound Kushen Injection.

(Fig. 4Aa). Consistent with previous findings, no fibrosis was noted in these mice (46). Hematoxylin and eosin stains of lung tissues derived from CKI-treated TLI mice (4 and 8 ml/kg) showed that these animals had significantly lower degree of RILI, which was demonstrated by minimal or mild interstitial pneumonia with infiltration of only a few inflammatory cells (Fig. 4Ab and c), that is in contrast with marked interstitial pneumonia in vehicle-treated TLI mice (Fig. 4Aa). Quantifications of the histopathological grade scores of lung lesions (Fig. 4B) showed a statistically significant reduction of RILI in CKI-treated (4 and 8 ml/kg) TLI mice in comparison with vehicle-treated TLI mice. These data indicate that CKI treatment substantially minimized the lung injuries caused by TLI in C3H mice.

*CKI reduced inflammatory cytokine levels in C3H mice after TLI.* Given inflammation is primarily associated with RILI, proinflammatory cytokines were measured in the serum of mice before and 72 h after irradiation. IL6 levels in the TLI + vehicle group (4.75±0.59 pg/ml) were 8.0-fold higher than in the nonirradiated control mice (0.58±0.38 pg/ml) (Fig. 5A). TLI + CKI (4 and 8 ml/kg) significantly reduced the mean IL6 levels to 1.09±0.15 pg/ml and 0.70±0.29 pg/ml (P<0.001; Fig. 5A), respectively, which were comparable to that of the nonirradiated control mice. Similarly, IL17A levels of TLI + CKI-treated mice (4 and 8 ml/kg) were 73% lower than that of TLI + vehicle control mice (P<0.01; Fig. S4); TGF-β levels of TLI + CKI-treated mice (4 and 8 ml/kg) were 42 and 60% lower than that of TLI + vehicle control mice (P<0.05; Fig. 5B).

Furthermore, to investigate the temporal change of cytokines in TLI mice, serum IL6 was measured at 2, 4 and 8 weeks after TLI and expression of TGF-β in lung tissues was measured at 2 weeks after TLI. Levels of serum IL6 in TLI vehicle control group were 2.5-fold higher (P<0.01) than that of non-radiation control mice at 2 weeks after TLI but recovered at 4 and 8 weeks. CKI 4 or 8 ml/kg treated mice

showed stable low levels of IL6 at 2, 4, and 8 weeks after TLI (Fig. 5C). Consistently, IHC staining in lung tissues at 2 weeks after TLI showed that the percent of TGF-β positive cells in the lung tissues of CKI 8 ml/kg treated mice were significantly lower than that of vehicle control mice (2.5% vs. 26.9%, P=0.005) (Fig. 5D and E). These data suggest that CKI markedly decreased radiation-induced inflammatory cytokine levels and exerted anti-inflammatory activity as an early response to radiation.

*CKI modulated COX-2 activity and COX-2 metabolites in the lung tissues of C3H mice after TLI.* COX-2 metabolites and COX-2 activity were assessed in the lung tissues of mice 4 weeks after radiation. As shown in Fig. 6A, there were significantly lower levels of the intralung COX-2 metabolites $PGD_2$ and $PGE_2$ 4 weeks after radiation in the CKI-treated (4 and 8 ml/kg) mice compared to the vehicle control mice (P<0.05). To understand whether this reduction of COX-2 metabolites was mediated by suppression of COX-2 activity or protein expression, COX-2 activity and protein expression were measured by ELISA, IHC staining and western blot in irradiated lung tissues. The COX-2 activity was significantly reduced at 4 weeks after radiation in the lung tissues of CKI (4 and 8 ml/kg) treated mice compared to that of vehicle control mice (P<0.05, Fig. 6B). In contrast, the percentages of COX-2-positive cells and COX-2 protein expression in the irradiated lung tissues were similar between CKI treated mice and vehicle control (Fig. S5), suggesting that the reduction in COX-2 metabolites by CKI was not due to inhibition of COX-2 protein expression.

To further understand whether CKI also affects the degradation pathway of prostaglandins, the protein level of 15-PGDH, which is the common degradation enzyme of $PGE_2$ and $PGD_2$, was examined in the lung tissues of C3H mice (Fig. 6C). CKI (8 ml/kg) treatment significantly upregulated the expression of 15-PGDH compared to that of vehicle control group (P=0.014) (Fig. 6D). These results suggest that CKI elicited reduction of $PGE_2$ and $PGD_2$ could be at least
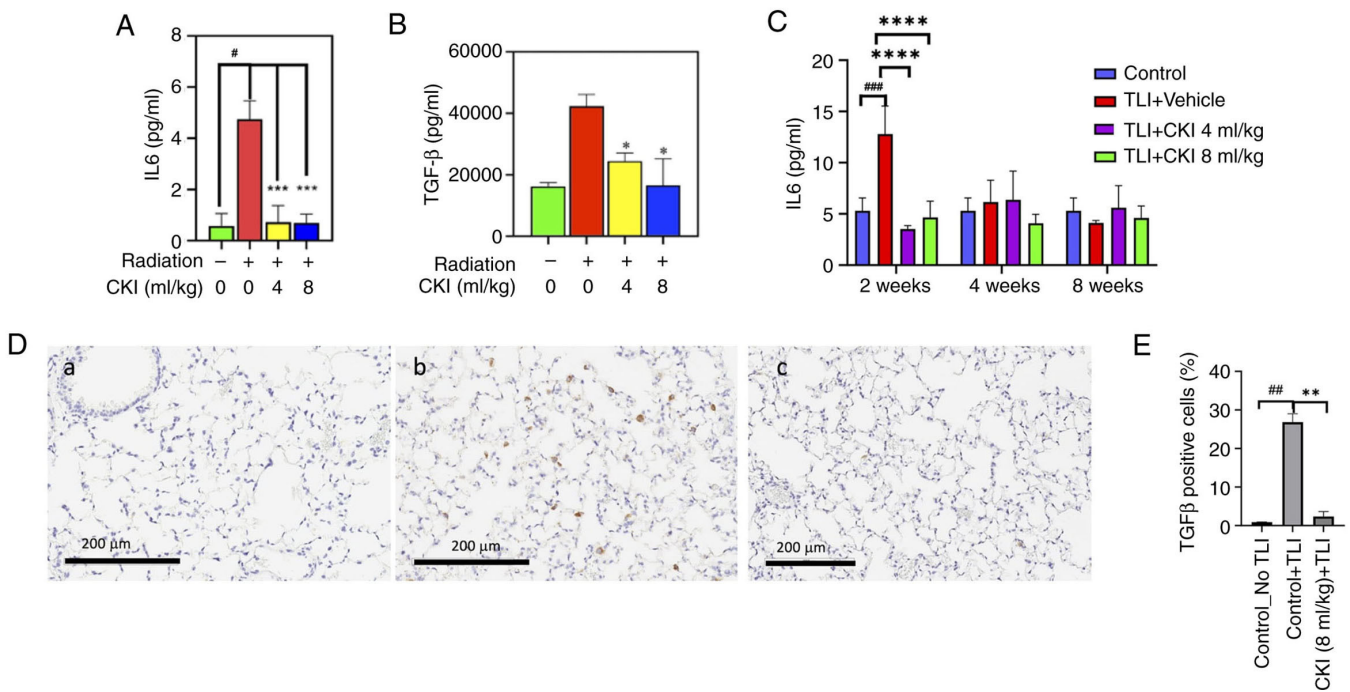
Figure 5. Proinflammatory cytokines in serum and lung tissues of C3H mice treated with TLI with or without CKI. Serum cytokine levels of: (A) IL6 and (B) TGF-β at 72 h after concurrent 13.5 Gy TLI with vehicle control or CKI treatment (n=3-4 per group). Measurements were made using ELISA. (C) Serum levels of IL6 at 2, 4 and 8 weeks after 13.5 Gy TLI with vehicle control or CKI treatment (n=3-4 per group). (D) Immunohistochemistry analysis of TGF-β in lung tissues of C3H mice at 2 weeks after treatment (scale bars, 200 $\mu$m): (a) Normal, (b) TLI (13.5 Gy) and (c) TLI + CKI (8 ml/kg). (E) Quantitative analysis of TGF-β-positive cells in lung tissues. Data are presented as the mean ± standard deviation. *P<0.05, **P<0.01, ***P<0.001 and ****P<0.0001 vs. irradiated vehicle control. #P<0.05, ##P<0.01 and ###P<0.001 vs. normal non-irradiated control. TGF-β, transforming growth factor β; CKI, Compound Kushen Injection; TLI, total lung irradiation.
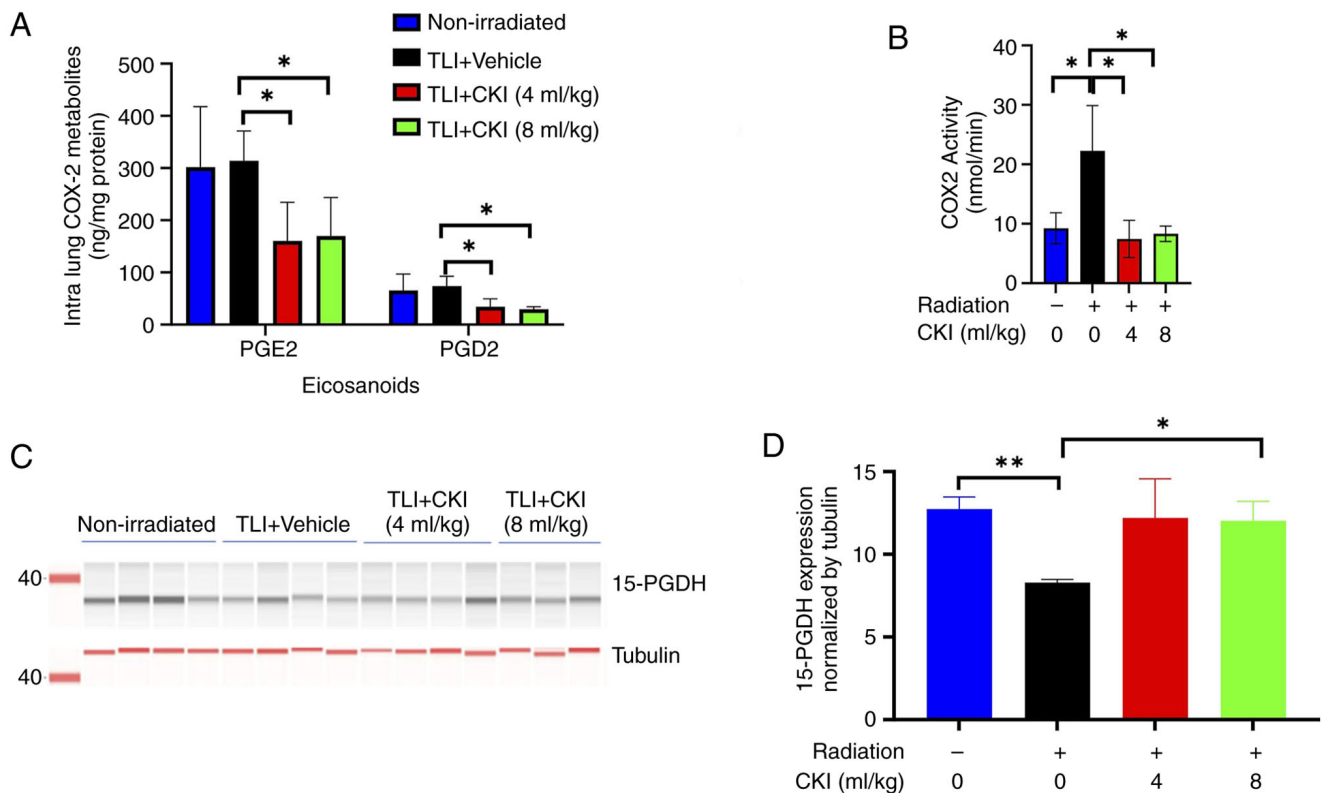


Figure 6. Effect of CKI on the COX-2 metabolic pathway. (A) The intralung COX-2 metabolites PGD$_2$ and PGE$_2$ measured using liquid chromatography/tandem mass spectrometry. (B) COX-2 activity measured by ELISA kit. (C) Western blot analysis (D) and quantification of 15-PGDH protein expression in lung tissues of C3H mice at 4 weeks after TLI with vehicle control or CKI treatment. Data are presented as mean ± standard deviation. COX-2 activity data was log-transformed for analysis as non-normal distribution. *P<0.05 and **P<0.01. CKI, Compound Kushen Injection; COX-2, cyclooxygenase 2; PGE$_2$, prosta-glandin E$_2$; PGD$_2$, prostaglandin D2; 15-PGDH, 15-hydroxyprostaglandin dehydrogenase; RT, radiation therapy.

partially due to inhibition of COX-2 activity and increase in the degradation of these metabolites in irradiated lung tissues.

## Discussion

In the present study, we provided several lines of evidence to suggest that CKI reduces inflammation and alleviates radiation-induced pneumonitis. First, pre-irradiation or concurrent TLI and CKI 8 ml/kg was associated with improved survival of irradiated C3H mice. Second, CKI was associated with reduced incidence and severity of RILI evaluated by micro-CT imaging and histopathology. To our knowledge, this is the first demonstration of CKI's preventive effect on RILI in C3H mice. Third, CKI treatment significantly reduced key proinflammatory cytokines including IL6, IL17, and TGF-β as well as activity of COX-2 supporting anti-inflammation as the hypothesized mechanism of action of CKI.

RILI generally occurs in two main phases: an early inflammatory phase, called RP, which is characterized by immune cell infiltration and cytokine release, and a late fibrotic phase, during which tissue remodeling and fibrosis result in chronic lung dysfunction. Cytokines such as IL-6, TGF-β, and IL17 have been demonstrated to play key roles in mediating the inflammatory response. For example, a study has shown that the levels of the circulating proinflammatory cytokines such as IL6 in serum and BAL were correlated with tissue levels of the proinflammatory markers (17). In addition, higher plasma levels of inflammatory cytokines detected quickly within 48 h after radiation, such as TGF-β1, IL1α, and IL6, predict a higher risk for RILI (19,21,22,47). It emphasizes the important role of activation of these proinflammation cytokines and related pathways in RILI. Interestingly, anti-inflammatory drugs such as dexamethasone and an anti-IL17A antibody reduced the concentrations of IL17A (25,48,49), TGF-β, and IL6, and alleviated RILI and subsequent fibrosis in mice, suggesting the importance of IL17A in inflammation and fibrosis (49). The current data demonstrated that CKI significantly reduced radiation-induced elevation of multiple key pro-inflammatory cytokines including IL6, IL17A, and TGF-β in the serum of C3H mice 72 h after irradiation. The findings also revealed that the levels of TGF-β in the lung tissues of CKI-treated mice were significantly reduced at 2 weeks after irradiation, which is consistent with a recently published mechanism study (50). However, which of the three inflammatory cytokines, or perhaps others, are the key regulatory factors is not clear. As the inflammatory response is complex and multidimensional, it is unlikely that there is one specific component driving the effects. Examining the regulatory pathway for the changes of these cytokines or perhaps others mediating the CKI-elicited protective effects in RILI deserves further investigation.

Prostaglandins, known inflammatory mediators, are synthesized from arachidonic acid via the actions of cyclooxygenase (COX-1 or COX-2) enzymes and degraded by the key enzyme 15-PGDH (51). Thus, the levels of prostaglandins, especially $PGE_2$, are regulated by the COX-2 and 15-PGDH enzymes in tissues, including lung tissue (52). The current study found that CKI-treated mice had a decrease in COX-2 metabolites in irradiated lung tissues, including $PGD_2$ and $PGE_2$, suggesting that CKI may reduce RILI by targeting COX-2 pathways.

A prior study found that Clarithromycin prevented RILI by downregulating COX-2 protein expression in irradiated C57B/L6 mice (53). In our study, the results showed that CKI treatment did not reduce radiation-induced COX-2 expression but inhibited COX-2 activity, suggesting CKI reduced the intralung COX-2 metabolites ($PGD_2$ and $PGE_2$) through inhibiting COX-2 activity but not downregulating COX-2 protein expression. CKI treatment also led to upregulation of 15-PGDH expression, which could at least in part contribute to the CKI-elicited degradation of prostaglandins ($PGE_2$ and $PGD_2$). Given research has shown that 15-PGDH is abundant in both normal mouse and human lung tissues (54) and 15-PGDH has been demonstrated as a tumor suppressor in lung and colon cancer (55-58), it would be interesting to further understand how CKI is able to upregulate 15-PGDH levels in TLI mice and reduce overall RILI. Additionally, studies reported that COX-2 expression could be induced by TGF-β through TGF-β-TGFBR1-COX-2 signaling pathway (59-61) and transcriptionally regulated by NF-kB (62). Examination of NF-kB in the CKI treated TLI mice might help further understand the mechanism of action of CKI in RILI.

One of the limitations of the current series of experiments is not knowing which of the purported active components of CKI exerts the protective effects on RILI. Preclinical studies have demonstrated that matrine, one of the active ingredients in CKI, significantly improves the survival of mice with lipopolysaccharide-induced acute lung injuries and alleviates pulmonary edema by inhibiting inflammatory cytokines and mediators such as tumor necrosis factor α, IL6, and high mobility group protein B1 (38), and downregulating inflammatory genes such as *IL6*, *CCL1*, and *COX2* (63). Oxymatrine, another major component of CKI, has anti-inflammatory activity; however, studies have produced mixed results regarding its role in inhibiting cytokine levels and cytokine-cytokine receptor interactions in cancer cells (64,65). The flavonoids from kushen roots have been reported to significantly inhibit IL6, COX-2, and nitric oxide synthase in lipopolysaccharide-treated RAW 264.7 mouse macrophage cells and to suppress inflammation in a mouse arthritis model (66). However, which bioactive components (i.e., alkaloids, flavonoids) in CKI are responsible for CKI's protective effects against RILI remain unknown. Even though one can speculate that CKI's role in preventing RILI may be due to both alkaloids and flavonoids, further studies are needed to explore the specific components or combination that leads to CKI-induced reduction of RILI.

Previous studies have shown that micro-CT can be used for early detection and assessment of structural and histopathological changes of RILI in mice (67). Changes in micro-CT parameters (Hounsfield Units and pixels) of irradiated mouse lungs were highly correlated with histological changes, including air space enlargement, at 1 and 4 days post-irradiation (67). Plathow *et al* detected the development of radiation induced lung fibrosis prior to the onset of clinical parameters by monitoring the changes (increase in Hounsfield Units, intralobular opacity and fibrotic strandings) in micro-CT (68). In the current study, at least two physicians independently reviewed and evaluated micro-CT images of the lung for RILI changes before and after radiation. We observed that CKI 8 ml/kg treatment led to significantly less

RILI from 80% (vehicle control mice) to 8%. It was consistent with histopathology findings that CKI-treated mice had less interstitial pneumonitis and fewer inflammatory cell infiltrations compared to vehicle control mice. In addition, CKI itself did not cause any physiological changes in the normal lung tissues of C3H mice. This protective effect of CKI may have contributed to the longer survival of the CKI-treated mice.

However, the mice with minor or no RILI only had moderately longer survival than that of mice with RILI, suggesting that radiation-induced damage to other organs, such as esophagus and heart, may contribute to the mortality of mice without RILI. H&E-staining of heart tissue derived from irradiated mice with or without CKI treatment did not find any significant pathological changes in these tissues (data not shown) even though we did observe less macrophage infiltration in the lungs of CKI treated mice than that of vehicle control group. Yet, prior studies showed that CKI exhibited anti-tumor effect by activating proinflammatory responses and promoted tumor-associated macrophages and CD8+ T cells infiltration in tumor microenvironment (69,70). However, the current studies did not conduct a thorough evaluation of immune mechanisms or the effects of CKI on cancer growth, instead focusing on examining CKI's anti-inflammatory properties for the prevention of RILI. Other radiation-induced damage, such as thrombosis, bone marrow damage, and immune cell changes in TLI mice should be further investigated. Now that we have documented the anti-inflammatory effects of CKI in reducing RILI, future mechanistic studies could validate these findings with more in-depth studies using molecular inhibitors or activators and perform either transcriptomic or proteomic analysis to gain a more comprehensive understanding of CKI's effects.

Collectively, the current findings suggest that administering CKI-in a formulation and dosage similar to those routinely used clinically in China-improves survival and reduces the development of RILI in C3H mice. CKI treatment decreased expression of inflammatory cytokines, including TGF-β, IL6, and IL17, and reduced the activity and metabolites of intra-lung COX-2. These findings align with histopathological and micro-CT assessments, which demonstrated improvements in lung structure. Further clinical studies of CKI as a potential candidate for preventing RILI are warranted.

## Acknowledgements

## Funding

## Availability of data and materials

The data generated in the present study may be requested from the corresponding author.

## Authors' contributions

PY, TX, LC, DW and ZL developed the main conceptual ideas and provided input into the study design. MT, SC, BW, RR, PN and TX performed the experiments and numerical calculations for the planned experiments. MG evaluated the histological slides and facilitated data interpretation. TX, XX, LW and ZL evaluated the micro-CT images and facilitated data interpretation. PY and TX confirm the authenticity of all the raw data. SC, DW, PY, TX, LC, MG and ZXL drafted and/or reviewed the manuscript. All authors contributed to the manuscript at various stages, and have read and approved the final manuscript.

## Ethics approval and consent to participate

The animal research protocol (approval no. 00000955) was approved by the Institutional Animal Care and Use Committee of The University of Texas MD Anderson Cancer Center. All animal studies also comply with the ARRIVE guidelines and the AVMA euthanasia guidelines 2020.

## Patient consent for publication

Not applicable.

## Competing interests

The authors declare that they have no competing interests. Study drug, CKI, was provided by Shanxi Zhendong Pharmaceutical Co. (Changzhi, Shanxi, China).

## References

1. Jain V and Berman AT: Radiation pneumonitis: Old problem, new tricks. Cancers (Basel) 10: 222, 2018.
2. Rodrigues G, Lock M, D'Souza D, Yu E and Van Dyk J: Prediction of radiation pneumonitis by dose-volume histogram parameters in lung cancer-a systematic review. Radiother Oncol 71: 127-138, 2004.
3. Yan Y, Fu J, Kowalchuk RO, Wright CM, Zhang R, Li X and Xu Y: Exploration of radiation-induced lung injury, from mechanism to treatment: a narrative review. Transl Lung Cancer Res 11: 307-322, 2022.
4. Arroyo-Hernández M, Maldonado F, Lozano-Ruiz F, Muñoz-Montaño W, Nuñez-Baez M and Arrieta O: Radiation-induced lung injury: Current evidence. BMC Pulm Med 21: 9, 2021.
5. Yue J, Shi Q, Xu T, Jeter M, Chen TY, Komaki R, Gomez DR, Pan T, Cleeland CS, Liao Z and Wang XS: Patient-reported lung symptoms as an early signal of impending radiation pneumonitis in patients with non-small cell lung cancer treated with chemoradiation: An observational study. Qual Life Res 27: 1563-1570, 2018.
6. King TE Jr: Clinical advances in the diagnosis and therapy of the interstitial lung diseases. Am J Respir Crit Care Med 172: 268-279, 2005.
7. Trott KR, Herrmann T and Kasper M: Target cells in radiation pneumopathy. Int J Radiat Oncol Biol Phys 58: 463-469, 2004.
8. Tsoutsou PG and Koukourakis MI: Radiation pneumonitis and fibrosis: Mechanisms underlying its pathogenesis and implications for future research. Int J Radiat Oncol Biol Phys 66: 1281-1293, 2006.
9. Jin H, Yoo Y, Kim Y, Kim Y, Cho J and Lee YS: Radiation-induced lung fibrosis: preclinical animal models and therapeutic strategies. Cancers (Basel) 12: 1561, 2020.
10. Rades D, Fehlauer F, Bajrovic A, Mahlmann B, Richter E and Alberti W: Serious adverse effects of amifostine during radiotherapy in head and neck cancer patients. Radiother Oncol 70: 261-264, 2004.

11. Devine A and Marignol L: Potential of amifostine for chemo-radiotherapy and radiotherapy-associated toxicity reduction in advanced NSCLC: A meta-analysis. Anticancer Res 36: 5-12, 2016.
12. Roy S, Salerno KE and Citrin DE: Biology of radiation-induced lung injury. Semin Radiat Oncol 31: 155-161, 2021.
13. Liu XJ and Chen ZH: The pathophysiological role of mitochondrial oxidative stress in lung diseases. J Transl Med 15: 207, 2017.
14. Schieber M and Chandel NS: ROS function in redox signaling and oxidative stress. Curr Biol 24: R453-R462, 2014.
15. Giuranno L, Ient J, De Ruysscher D and Vooijs MA: Radiation-induced lung injury (RILI). Front Oncol 9: 877, 2019.
16. Lierova A, Jelicova M, Nemcova M, Proksova M, Pejchal J, Zarybnicka L and Sinkorova Z: Cytokines and radiation-induced pulmonary injuries. J Radiat Res 59: 709-753, 2018.
17. Ao X, Zhao L, Davis MA, Lubman DM, Lawrence TS and Kong FM: Radiation produces differential changes in cytokine profiles in radiation lung fibrosis sensitive and resistant mice. J Hematol Oncol 2: 6, 2009.
18. Hong JH, Chiang CS, Tsao CY, Lin PY, McBride WH and Wu CJ: Rapid induction of cytokine gene expression in the lung after single and fractionated doses of radiation. Int J Radiat Biol 75: 1421-1427, 1999.
19. Rübe CE, Wilfert F, Palm J, König J, Burdak-Rothkamm S, Liu L, Schuck A, Willich N and Rübe C: Irradiation induces a biphasic expression of pro-inflammatory cytokines in the lung. Strahlenther Onkol 180: 442-448, 2004.
20. Szabo S, Ghosh SN, Fish BL, Bodiga S, Tomic R, Kumar G, Morrow NV, Moulder JE, Jacobs ER and Medhora M: Cellular inflammatory infiltrate in pneumonitis induced by a single moderate dose of thoracic x radiation in rats. Radiat Res 173: 545-556, 2010.
21. Zhao L, Wang L, Ji W, Wang X, Zhu X, Hayman JA, Kalemkerian GP, Yang W, Brenner D, Lawrence TS and Kong FM: Elevation of plasma TGF-beta1 during radiation therapy predicts radiation-induced lung toxicity in patients with non-small-cell lung cancer: A combined analysis from Beijing and Michigan. Int J Radiat Oncol Biol Phys 74: 1385-1390, 2009.
22. Rube CE, Uthe D, Schmid KW, Richter KD, Wessel J, Schuck A, Willich N and Rube C: Dose-dependent induction of transforming growth factor beta (TGF-beta) in the lung tissue of fibrosis-prone mice after thoracic irradiation. Int J Radiat Oncol Biol Phys 47: 1033-1042, 2000.
23. Chen Y, Rubin P, Williams J, Hernady E, Smudzin T and Okunieff P: Circulating IL-6 as a predictor of radiation pneumonitis. Int J Radiat Oncol Biol Phys 49: 641-648, 2001.
24. Chen Y, Williams J, Ding I, Hernady E, Liu W, Smudzin T, Finkelstein JN, Rubin P and Okunieff P: Radiation pneumonitis and early circulatory cytokine markers. Semin Radiat Oncol 12 (1 Suppl 1): S26-S33, 2002.
25. Shaikh SB, Prabhu A and Bhandary YP: Interleukin-17A: A potential therapeutic target in chronic lung diseases. Endocr Metab Immune Disord Drug Targets 19: 921-928, 2019.
26. Baindara P: Targeting interleukin-17 in radiation-induced toxicity and cancer progression. Cytokine Growth Factor Rev 75: 31-39, 2024.
27. Paun A, Bergeron ME and Haston CK: The Th1/Th17 balance dictates the fibrosis response in murine radiation-induced lung disease. Sci Rep 7: 11586, 2017.
28. Hunter NR, Valdecanas D, Liao Z, Milas L, Thames HD and Mason KA: Mitigation and treatment of radiation-induced thoracic injury with a cyclooxygenase-2 inhibitor, celecoxib. Int J Radiat Oncol Biol Phys 85: 472-476, 2013.
29. Yang HJ, Youn H, Seong KM, Yun YJ, Kim W, Kim YH, Lee JY, Kim CS, Jin YW and Youn B: Psoralidin, a dual inhibitor of COX-2 and 5-LOX, regulates ionizing radiation (IR)-induced pulmonary inflammation. Biochem Pharmacol 82: 524-534, 2011.
30. Yang S: Ku Shen (Radix Sophorae Flavescentis). In: The Divine Farmer's Materia Medica: A Translation of the Shen Nong Ben Cao Jing. Yang Shou-zhong. Blue Poppy Press, Inc., Boulder, CO, USA, pp 56, 1998.
31. Zhou W, Wu J, Zhu Y, Meng Z, Liu X, Liu S, Ni M, Jia S, Zhang J and Guo S: Study on the mechanisms of compound Kushen injection for the treatment of gastric cancer based on network pharmacology. BMC Complement Med Ther 20: 6, 2020.
32. Wang S, Lian X, Sun M, Luo L and Guo L: Efficacy of compound Kushen injection plus radiotherapy on nonsmall-cell lungcancer: A systematic review and meta-analysis. J Cancer Res Ther 12: 1298-1306, 2016.

33. Ao M, Xiao X and Li Q: Efficacy and safety of compound Kushen injection combined with chemotherapy on postoperative Patients with breast cancer: A meta-analysis of randomized controlled trials. Medicine (Baltimore) 98: e14024, 2019.
34. Aung TN, Qu ZP, Kortschak RD and Adelson DL: Understanding the effectiveness of natural compound mixtures in cancer through their molecular mode of action. Int J Mol Sci 18: 656, 2017.
35. Deng B, Deng C and Cheng ZQ: Chinese herbal extractions for relieving radiation induced lung injury: A systematic review and meta-analysis. Evid Based Complement Alternat Med 2017: 2141645, 2017.
36. Liu J, Yu Q, Wang XS, Shi Q, Wang J, Wang F, Ren S, Jin J, Han B, Zhang W, et al: Compound kushen injection reduces severe toxicity and symptom burden associated with curative radiotherapy in patients with lung cancer. J Natl Compr Canc Netw 21: 821-830.e3, 2023.
37. Zhang J, Qu Z, Yao H, Sun L, Harata-Lee Y, Cui J, Aung TN, Liu X, You R, Wang W, et al: An effective drug sensitizing agent increases gefitinib treatment by down regulating PI3K/Akt/mTOR pathway and up regulating autophagy in non-small cell lung cancer. Biomed Pharmacother 118: 109169, 2019.
38. Zhang B, Liu ZY, Li YY, Luo Y, Liu ML, Dong HY, Wang YX, Liu Y, Zhao PT, Jin FG and Li ZC: Antiinflammatory effects of matrine in LPS-induced acute lung injury in mice. Eur J Pharm Sci 44: 573-579, 2011.
39. Cui J, Qu Z, Harata-Lee Y, Shen H, Aung TN, Wang W, Kortschak RD and Adelson DL: The effect of compound kushen injection on cancer cells: Integrated identification of candidate molecular mechanisms. PLoS One 15: e0236395, 2020.
40. Zhao Z, Fan H, Higgins T, Qi J, Haines D, Trivett A, Oppenheim JJ, Wei H, Li J, Lin H and Howard OM: Fufang Kushen injection inhibits sarcoma growth and tumor-induced hyperalgesia via TRPV1 signaling pathways. Cancer Lett 355: 232-241, 2014.
41. Williams JP, Brown SL, Georges GE, Hauer-Jensen M, Hill RP, Huser AK, Kirsch DG, Macvittie TJ, Mason KA, Medhora MM, et al: Animal models for medical countermeasures to radiation exposure. Radiat Res 173: 557-578, 2010.
42. Liao ZX, Travis EL and Tucker SL: Damage and morbidity from pneumonitis after irradiation of partial volumes of mouse lung. Int J Radiat Oncol Biol Phys 32: 1359-1370, 1995.
43. Travis EL: Relative radiosensitivity of the human lung. Adv Radiat Biol 12: 205-238, 1987.
44. Yang PY, Jiang Y, Rhea PR, Coway T, Chen D, Gagea M, Harribance SL and Cohen L: Human biofield therapy and the growth of mouse lung carcinoma. Integr Cancer Ther 18: 1534735419840797, 2019.
45. Yang PY, Chan D, Felix E, Madden T, Klein RD, Shureiqi I, Chen X, Dannenberg AJ and Newman RA: Determination of endogenous tissue inflammation profiles by LC/MS/MS: COX- and LOX-derived bioactive lipids. Prostaglandins Leukot Essent Fatty Acids 75: 385-395, 2006.
46. Dileto CL and Travis EL: Fibroblast radiosensitivity in vitro and lung fibrosis in vivo: Comparison between a fibrosis-prone and fibrosis-resistant mouse strain. Radiat Res 146: 61-67, 1996.
47. Finkelstein JN, Johnston CJ, Baggs R and Rubin P: Early alterations in extracellular matrix and transforming growth factor beta gene expression in mouse lung indicative of late radiation fibrosis. Int J Radiat Oncol Biol Phys 28: 621-631, 1994.
48. Wang LP, Wang YW, Wang BZ, Sun GM, Wang XY and Xu JL: Expression of interleukin-17A in lung tissues of irradiated mice and the influence of dexamethasone. ScientificWorldJournal 2014: 251067, 2014.
49. Wang BZ, Wang LP, Han H, Cao FL, Li GY, Xu JL, Wang XW and Wang LX: Interleukin-17A antagonist attenuates radiation-induced lung injuries in mice. Exp Lung Res 40: 77-85, 2014.
50. Yang Y, Sun M, Li W, Liu C, Jiang Z, Gu P, Li J, Wang W, You R, Ba Q, et al: Rebalancing TGF-β/Smad7 signaling via Compound kushen injection in hepatic stellate cells protects against liver fibrosis and hepatocarcinogenesis. Clin Transl Med 11: e410, 2021.
51. Howe LR, Subbaramaiah K, Brown AM and Dannenberg AJ: Cyclooxygenase-2: A target for the prevention and treatment of breast cancer. Endocr Relat Cancer 8: 97-114, 2001.
52. Yang P, Chan D, Felix E, Cartwright C, Menter DG, Madden T, Klein RD, Fischer SM and Newman RA: Formation and antiproliferative effect of prostaglandin E(3) from eicosapentaenoic acid in human lung cancer cells. J Lipid Res 45: 1030-1039, 2004.
53. Lee SJ, Yi CO, Heo RW, Song DH, Cho YJ, Jeong YY, Kang KM, Roh GS and Lee JD: Clarithromycin attenuates radiation-induced lung injury in mice. PLoS One 10: e0131671, 2015.

54. Smith JNP, Witkin MD, Jogasuria AP, Christo KF, Raffay TM, Markowitz SD and Desai AB: Therapeutic targeting of 15-PGDH in murine pulmonary fibrosis. Sci Rep 10: 11657, 2020.

55. Myung SJ, Rerko RM, Yan M, Platzer P, Guda K, Dotson A, Lawrence E, Dannenberg AJ, Lovgren AK, Luo G, *et al*: 15-Hydroxyprostaglandin dehydrogenase is an in vivo suppressor of colon tumorigenesis. Proc Natl Acad Sci USA 103: 12098-12102, 2006.

56. Tai HH, Tong M and Ding Y: 15-Hydroxyprostaglandin dehydrogenase (15-PGDH) and lung cancer. Prostaglandins Other Lipid Mediat 83: 203-208, 2007.

57. Ding Y, Tong M, Liu S, Moscow JA and Tai HH: NAD+-linked 15-hydroxyprostaglandin dehydrogenase (15-PGDH) behaves as a tumor suppressor in lung cancer. Carcinogenesis 26: 65-72, 2005.

58. Yan M, Rerko RM, Platzer P, Dawson D, Willis J, Tong M, Lawrence E, Lutterbaugh J, Lu S, Willson JK, *et al*: 15-Hydroxyprostaglandin dehydrogenase, a COX-2 oncogene antagonist, is a TGF-beta-induced suppressor of human gastrointestinal cancers. Proc Natl Acad Sci USA 101: 17468-17473, 2004.

59. Chai Y, Lam RKK, Calaf GM, Zhou H, Amundson S and Hei TK: Radiation-induced non-targeted response in vivo: Role of the TGFβ-TGFBR1-COX-2 signalling pathway. Br J Cancer 108: 1106-1112, 2013.

60. Fang L, Chang HM, Cheng JC, Leung PCK and Sun YP: TGF-β1 induces COX-2 expression and PGE2 production in human granulosa cells through Smad signaling pathways. J Clin Endocrinol Metab 99: E1217-E1226, 2014.

61. Farhood B, Khodamoradi E, Hoseini-Ghahfarokhi M, Motevaseli E, Mirtavoos-Mahyari H, Eleojo Musa A and Najafi M: TGF-β in radiotherapy: Mechanisms of tumor resistance and normal tissues injury. Pharmacol Res 155: 104745, 2020.

62. Lee S, Shin S, Kim H, Han S, Kim K, Kwon J, Kwak JH, Lee CK, Ha NJ, Yim D and Kim K: Anti-inflammatory function of arctiin by inhibiting COX-2 expression via NF-κB pathways. J Inflamm (Lond) 8: 16, 2011.

63. Liou CJ, Lai YR, Chen YL, Chang YH, Li ZY and Huang WC: Matrine attenuates COX-2 and ICAM-1 expressions in human lung epithelial cells and prevents acute lung injury in LPS-induced mice. Mediators Inflamm 2016: 3630485, 2016.

64. Aung TN, Nourmohammadi S, Qu Z, Harata-Lee Y, Cui J, Shen HY, Yool AJ, Pukala T, Du H, Kortschak RD, *et al*: Fractional deletion of compound kushen injection indicates cytokine signaling pathways are critical for its perturbation of the cell cycle. Sci Rep 9: 14200, 2019.

65. Xu GL, Yao L, Rao SY, Gong ZN, Zhang SQ and Yu SQ: Attenuation of acute lung injury in mice by oxymatrine is associated with inhibition of phosphorylated p38 mitogen-activated protein kinase. J Ethnopharmacol 98: 177-183, 2005.

66. Jin JH, Kim JS, Kang SS, Son KH, Chang HW and Kim HP: Anti-inflammatory and anti-arthritic activity of total flavonoids of the roots of Sophora flavescens. J Ethnopharmacol 127: 589-595, 2010.

67. Saito S and Murase K: Detection and early phase assessment of radiation-induced lung injury in mice using micro-CT. PLoS One 7: e45960, 2012.

68. Plathow C, Li M, Gong P, Zieher H, Kiessling F, Peschke P, Kauczor HU, Abdollahi A and Huber PE: Computed tomography monitoring of radiation-induced lung fibrosis in mice. Invest Radiol 39: 600-609, 2004.

69. Yang Y, Sun M, Yao W, Wang F, Li X, Wang W, Li J, Gao Z, Qiu L, You R, *et al*: Compound kushen injection relieves tumor-associated macrophage-mediated immunosuppression through TNFR1 and sensitizes hepatocellular carcinoma to sorafenib. J Immunother Cancer 8: e000317, 2020.

70. Liu X, Bai M, Li H, Ye P, Duan X, Wu C, Huang Z, Lu S, Zhang J, Zhao Z, *et al*: Single-cell RNA-sequencing uncovers compound kushen injection synergistically improves the efficacy of chemotherapy by modulating the tumor environment of breast cancer. Front Immunol 13: 965342, 2022.